

Effect of silica fume and gypsum on properties of Mg-based hydraulic lime

Moon-Kwan Choi^{a,c}, Ki-Yeon Moon^{a,c}, Jin-Sang Cho^a, Kye-Hong Cho^a, Ji-Whan Ahn^b and Soon-Chul Ur^c

^aDepartment of Research and Development, Korea Institute of Limestone and Advanced Materials, 18-1 Udeok-gil, Maepo-eup, Danyang, Chungbuk 27003, Korea

^bMineral Resources Research Division, Korea Institute of Geoscience and Mineral Resources, 124 Gwahak-ro, Yuseong-gu, Daejeon, 34132, Korea

^cDepartment of Materials Science and Engineering, Korea National University of Transportation, 50 Deahangno, Chungju, Chungbuk 27469, Korea

In the present study, to improve the properties of Mg-based hydraulic lime prepared by using Korean low-grade dolomite, inorganic admixtures such as silica fume and gypsum were mixed with the dolomite, and the properties of the resulting hydraulic lime were evaluated depending on the amount of admixtures and the curing time. The silica fume mixing ratio was 10%, 20%, and 30%, and the gypsum mixing ratio was 0% and 3%. The samples, prepared as a paste and a mortar, were cured at a temperature of 20 °C and a humidity of 95% for 3, 7, 28, 56, and 91 days. The hydration characteristics and the physical properties of the samples at each curing time were evaluated. The experimental results showed an increase of C-S-H production was increased with increasing silica fume mixing ratio and curing time. The quantity of C-S-H produced was greater in the samples prepared without mixing gypsum. The measurement of the compressive strength showed that the strength was decreased at a silica fume mixing ratio higher than a certain level regardless of the mixing of gypsum. The strength was less decreased in the samples prepared by mixing gypsum. The best properties were found in the sample prepared by mixing 20% silica fume and 3% gypsum.

Key words: Dolomitic low grade limestone, Mg-base hydraulic lime, Silica fume, Gypsum, Hydration.

Introduction

Previous reports have shown that dolomite plaster mixed with materials such as sand, rice straw, and cement has good applicability, but few reports about actual applications can be found because an Mg-based lime binder using dolomite may undergo cracking generated by the expansion during the curing process due to the high MgO content or by the contraction during the dry curing process [1].

According to the EU standards, lime binders are classified as nonhydraulic lime and hydraulic lime [2-3]. Mg-based lime binders are non-hydraulic lime and classified into four types with reference to the MgO and CaO content [2]. General hydraulic lime is Ca-based hydraulic lime, such as NHL and HL, in which CaO, C₃A, C₂S, and C₃S are present together, and the EU standards specify as necessary property test items the compressive strength, particle size, free water, penetration resistance, air content, and setting. On the contrary, the specified necessary test properties for Mg-based non-hydraulic lime include only the items related to particle size, free water, penetration resistance, and

air content [2-3]. This is because of the difference in the mineral compositions: the durability and the physical property stability are lower in the non-hydraulic lime than in the hydraulic lime since the curing characteristics of the non-hydraulic lime are dependent only on the carbonation. In actual work sites, hydraulic lime having better physical properties with regard to compressive strength and setting time is applied more frequently [4-5].

Recently, some researchers have suggested that the curing characteristics of Mg-based lime binder may be semi-hydraulic, predicting that long-term stability in the contraction and expansion of hardened matrix may be secured if Mg-based lime binders is prepared as a hydraulic lime [1, 6-8].

In the present study, as a method of increasing the applicability of Mg-based hydraulic lime prepared with Korea low-grade dolomite (dolomitic natural hydraulic lime; D-NHL) satisfying the EU standards of hydraulic lime properties, inorganic admixtures were added to the lime. The change in the properties and the factors to the property expression were investigated experimentally with the prepared D-NHL.

Experimental

Properties of raw materials

*Corresponding author:
Tel : +82-43-422-2094
Fax: +82-43-422-5581
E-mail: chsang@kilam.re.kr

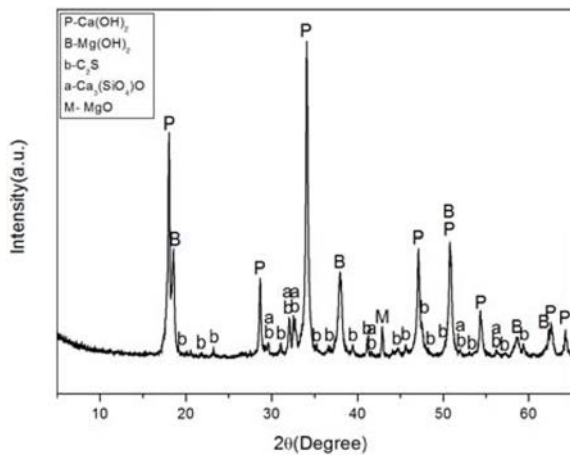


Fig. 1. XRD patterns of Mg-base hydraulic lime.

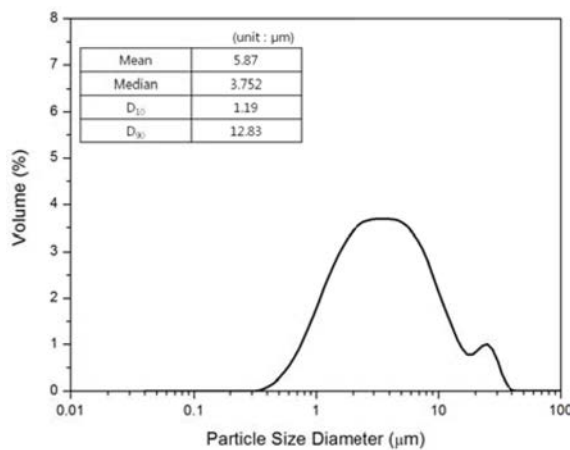


Fig. 2. Particle size distribution of Mg-base hydraulic lime.

Fig. 1 shows the XRD pattern of the D-NHL prepared by calcinating of low-grade dolomite, having a size of 20 to 30 mm, in an electric furnace at 1250 °C for two hours, and then performing hydration and pulverization, indicating that the major mineral compositions were $\text{Ca}(\text{OH})_2$, $\text{Mg}(\text{OH})_2$, C_2S , C_3S , and remaining MgO . The difference in the mineral compositions between non-hydraulic lime and hydraulic lime is the presence of hydraulic mineral compositions such as C_2S , C_3S , C_3A , and C_4AF . In the D-NHL prepared in the present study, hydraulic mineral compositions such as C_2S and C_3S were found, indicating that the properties may be hydration reaction. The mean particle size of the D-NHL particles pulverized with an air-jet mill was 5.87 μm , which was smaller than the upper limit of the EU standards (90 μm) (Fig. 2).

Inorganic admixtures

Table 1 and Fig. 3 shows the results of a chemical analysis and an XRD analysis of the silica fume (SF) and gypsum that were used to improve the properties of D-NHL. The analysis of the mineral and the chemical composition of the inorganic admixtures

Table 1. Chemical analysis of silica fume and gypsum.

	SF	Gypsum
Na_2O	0.09	0.03
MgO	0.75	0.31
Al_2O_3	0.10	0.61
SiO_2	95.49	1.37
P_2O_5	0.18	0.01
SO_3	0.64	51.0
K_2O	1.72	0.09
CaO	0.63	42.2
MnO	0.05	–
Fe_2O_3	0.04	0.18

(unit : %, by weight).

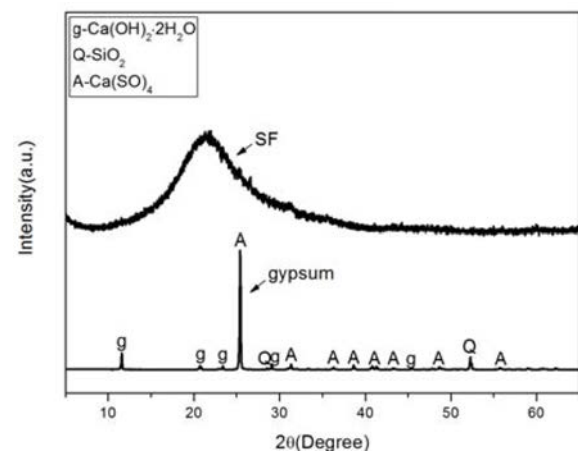


Fig. 3. XRD patterns of silica fume and gypsum.

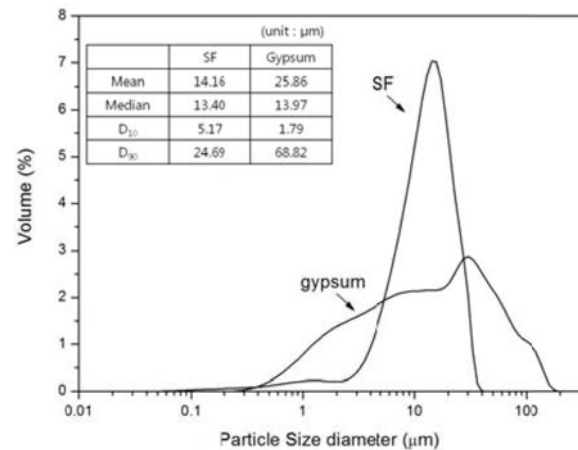


Fig. 4. Particle size distribution of silica fume and gypsum.

revealed that the main component of SF was amorphous SiO_2 (over 95%) and the content of other materials except SiO_2 was extremely low. The main components of gypsum were CaO and SO_3 (42.2% and 51%, respectively). The major mineral composition was anhydrous gypsum, while a small amount of dihydrate gypsum was also included.

The mean particle sizes of SF and gypsum was

14 μm and 25 μm (Fig. 4), and thus the SF and gypsum particles were larger than the D-NHL particles shown in Fig. 2. The density of the SF particle size was high at around 10 μm .

Experimental Methods

Experiment with Paste

Pastes of D-NHL were prepared to investigate the curing characteristics of the D-NHL hardened matrix depending on the inorganic admixture addition, and the behavior of the properties depending on the amount of added admixtures and the curing was verified by observing the change in the mineral compositions. For the analysis of the mineral compositions, an X-ray diffraction (XRD; D/max 2500V/P, Rigaku Co. Ltd. Japan) analysis, a differential scanning calorimeter (DSC; STA 449C Jupiter, Netzsch Co, Ltd. Germany) analysis, and porosity measurement (Auto Pore IV 9520, Micromeritics Co. Ltd. USA) were performed. Table 2 and Table 3 show the experimental conditions as well as the designation of the samples.

Experiment with Mortar

To investigate the expression of the strength performance depending on the amount of mixed inorganic admixtures, D-NHL mortar samples were prepared. First pre-mixing with the inorganic admixtures, each sample was prepared as a mortar at a ratio of D-NHL (+ admixture) : sand : water = 1 : 3 : x (flow (165 \pm 3) mm) according to the BS EN 459-2:2015. The samples were cured at a temperature of 20 $^{\circ}\text{C}$ and a relative humidity of 95%, and the compressive strength

of the individual samples was measured at each curing. The rate of loading during the measurement of the compressive strength was 144 kN/min, and the mortar preparation conditions and the sample designation was the same as the paste samples described above (Table 2 and Table 3).

Experimental Results

Fig. 5 show the XRD analysis results of the D-NHL paste depending on the SF mixing, representing the change of the mineral compositions depending on the amount of the SF addition. The results showed that the major mineral compositions were $\text{Ca}(\text{OH})_2$, $\text{Mg}(\text{OH})_2$, CaCO_3 , C_2S , and unreacted MgO . The kinds of mineral compositions produced were similar regardless of the amount of the added SF.

In all the samples, $\text{Ca}(\text{OH})_2$ was decreased and CaCO_3 was increased, as the material age was increased. CaCO_3 was produced by carbonation of $\text{Ca}(\text{OH})_2$. When $\text{Ca}(\text{OH})_2$ is converted into CaCO_3 , crystal growth occurred, which densifies the internal structure of a hardened matrix to improve the durability [1, 3]. Since the production of CaCO_3 was continuously increased with curing. Thus long-term improvement of the properties may be expected through the carbonation of $\text{Ca}(\text{OH})_2$. However, a change of the mineral compositions by the reaction of $\text{Mg}(\text{OH})_2$ was not observed, further studies and detailed instrumental analyses may need to be conducted in this regard [8].

C_2S is a major hydraulic mineral composition existing in D-NHL, and the presence of the mineral phase was verified through XRD. However, no compound produced by the hydration of C_2S was found until the curing of 91 days. In addition, the production of calcium silicate-based hydrates by pozzolanic reaction of silica fume was not accurately investigated.

An XRD analysis was performed with the D-NHL paste prepared by mixing SF and gypsum (Fig. 6). The major mineral compositions were $\text{Ca}(\text{OH})_2$, $\text{Mg}(\text{OH})_2$, CaCO_3 , C_2S , unreacted MgO , and remaining gypsum CaSO_4 and $\text{CaSO}_4 \cdot 2\text{H}_2\text{O}$. Unreacted gypsum may contribute to the improvement of the properties of the hardened matrix by filler, but it may decrease the reactivity [9-11]. Thus, the change of the properties may need to be investigated for a longer period of time.

For a more accurate investigation of the mineral compositions identified by the XRD analysis, a DSC analysis was performed. The DSC results of the D-NHL prepared by mixing SF (Fig. 7) showed an endothermic peak representing C-S-H hydrates around 120 $^{\circ}\text{C}$, an endothermic peak representing $\text{Mg}(\text{OH})_2$ around 400 $^{\circ}\text{C}$, an endothermic peak representing $\text{Ca}(\text{OH})_2$ around 500 $^{\circ}\text{C}$, and an endothermic peak representing the decarbonation of CaCO_3 around 800 $^{\circ}\text{C}$. Although not found in the XRD analysis, the production of calcium

Table 2. Experimental condition of D-NHL samples.

Raw material	Mg-base hydraulic lime (D-NHL)
SF mixing ratio	(10, 20, 30) %
Gypsum mixing ratio	(0, 3) %
Water ratio	Paste: 60 (by weight) Mortar: Flow (165 \pm 3) mm
Curing condition	Temperature 20 $^{\circ}\text{C}$, relative humidity 95%
Curing	(3, 7, 28, 56, 91) days

Table 3. Sample designation of D-NHL samples.

SF mixing ratio	Gypsum	Sample designation
10%		D-SF10
20%	0%	D-SF20
30%		D-SF30
10%		D-SF10-g
20%	3%	D-SF20-g
30%		D-SF30-g

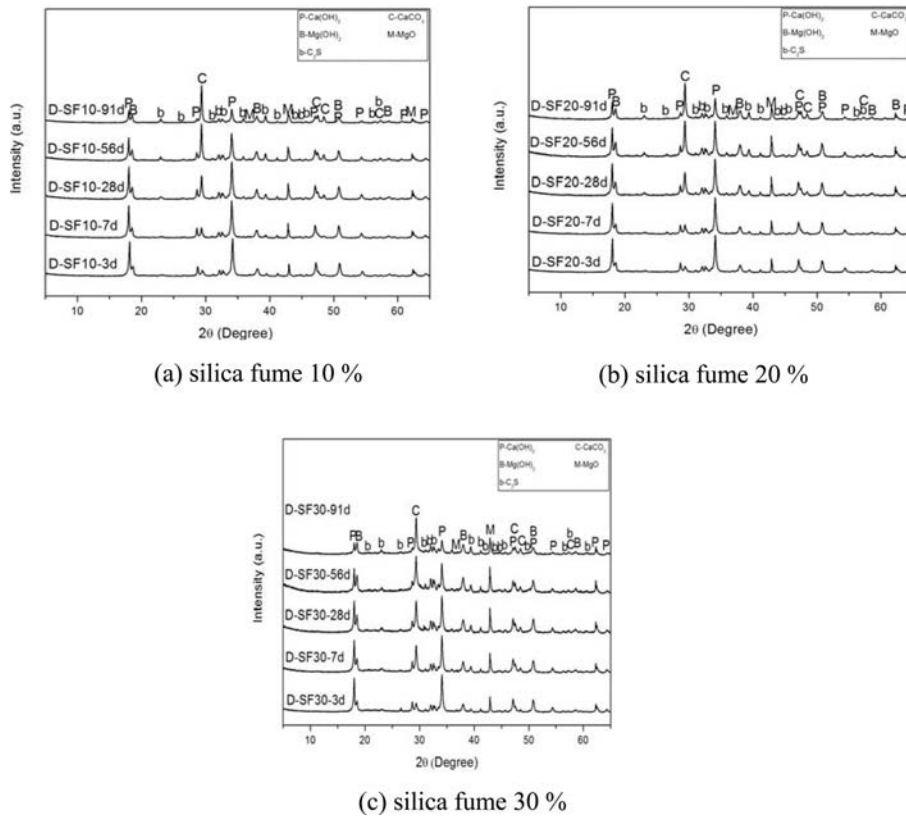


Fig. 5. XRD patterns of Mg-based hydraulic lime containing silica fume.

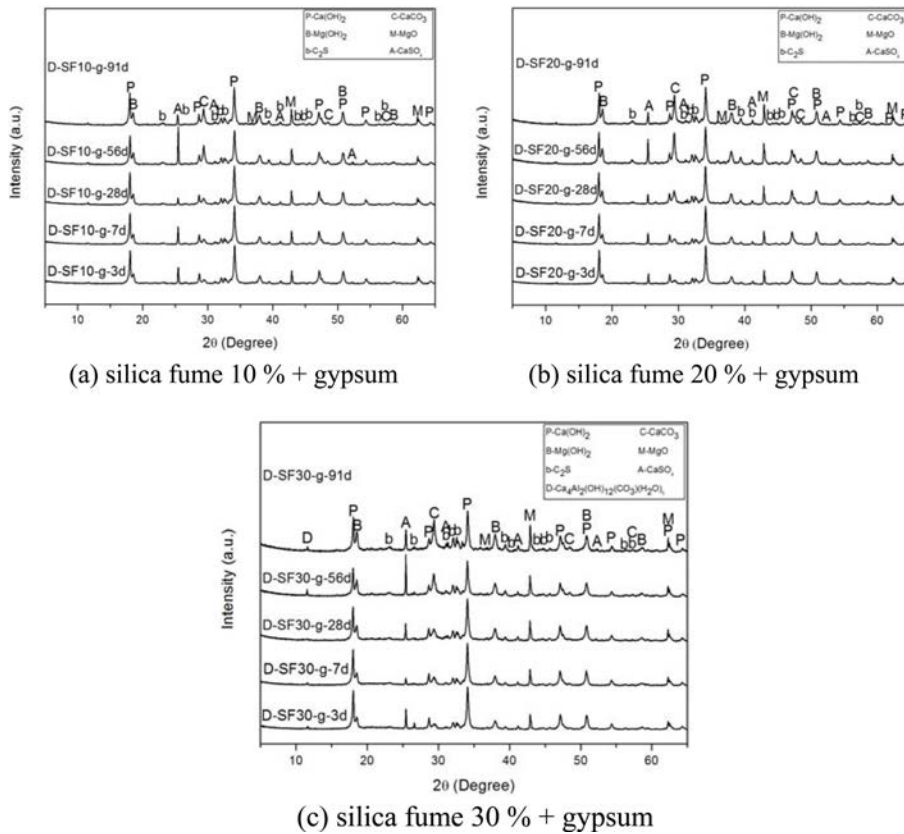


Fig. 6. XRD patterns of Mg-based hydraulic lime containing silica fume and gypsum.

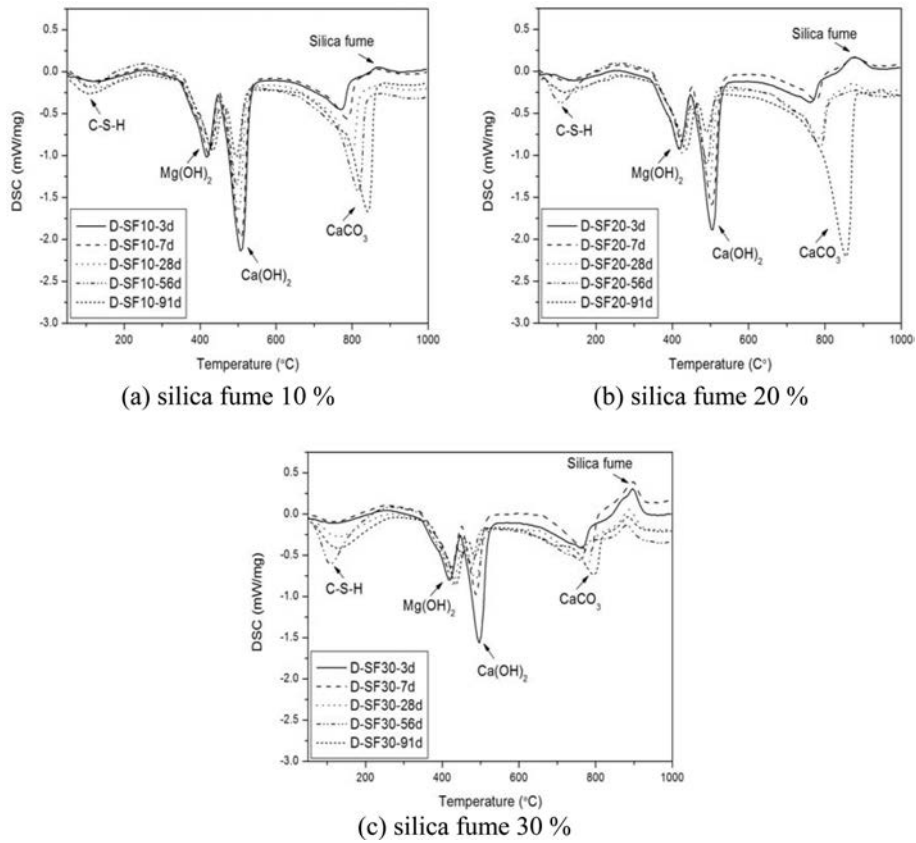


Fig. 7. DSC curves of Mg-based hydraulic lime containing silica fume.

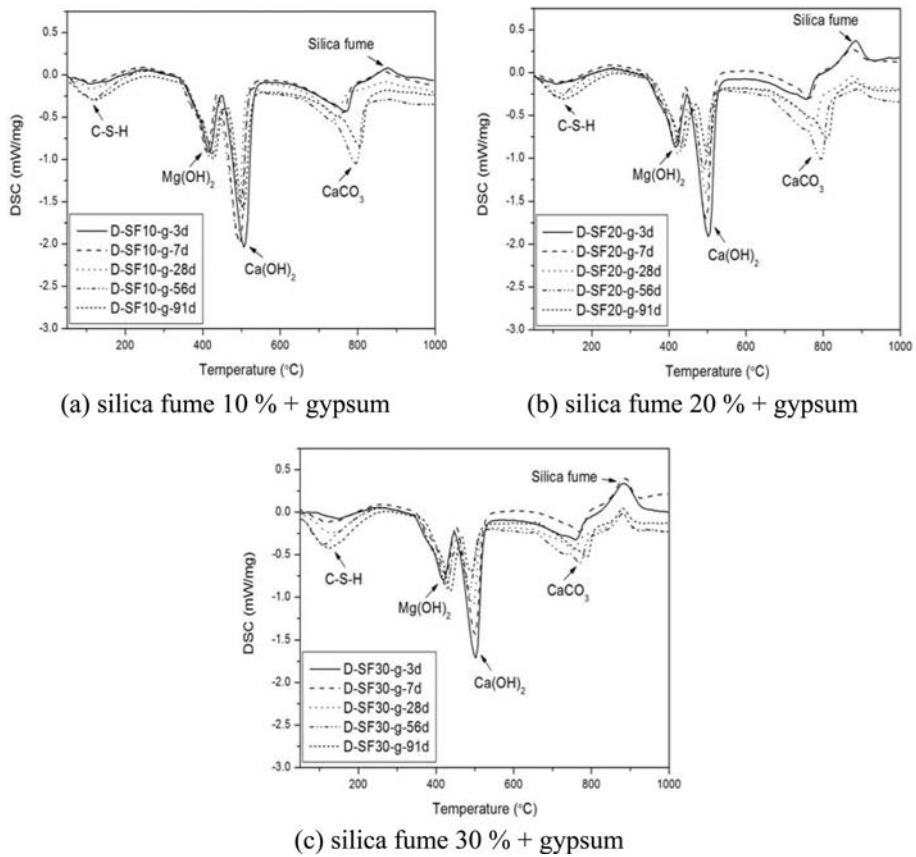


Fig. 8. DSC curves of Mg-based hydraulic lime containing silica fume and gypsum.

silicate based hydrates was increased as the amount of mixed SF was increased (around 120 °C). In addition, the overall production of the hydrates was increased as the curing was increased. The peak representing the de-carbonation (around 800 °C) was greater at a longer curing, indicating that the carbonation occurred continuously with curing.

The peak representing $\text{Ca}(\text{OH})_2$ at around 500 °C decreased as the material age and the amount of added SF increased. The CaCO_3 peak shown in Fig. 7(a) was smaller than the CaCO_3 peak shown in Fig. 7(c), which may be because $\text{Ca}(\text{OH})_2$ contributes more to the hydration reaction than to the carbonation.

The DSC results of the D-NHL prepared by mixing SF and gypsum (Fig. 8) showed a trend similar to that of the peaks shown in Fig. 7. The change of the produced mineral compositions by the mixing of gypsum was not significant. However, the peak representing the C-S-H hydrates at around 120 °C and the peak representing the de-carbonation of CaCO_3 at around 800 °C were smaller in the samples prepared by mixing gypsum than in the samples prepared without mixing gypsum. Overall, the quantity of the reaction products was smaller in the samples prepared by mixing gypsum than in the samples prepared without gypsum. Since SF is not reacts with gypsum, the mixed gypsum may have remained in the hardened matrix and acted as a filler. Hence, the internal pore structure was denser in the samples prepared by mixing SF and gypsum together than in the samples prepared by mixing only SF. As a result, since the CO_2 absorption was more difficult, the CaCO_3 production was less and the hydration was delayed, the amounts of the hydration and carbonation reaction products were smaller than in the samples by mixing only SF [12-13].

The XRD and DSC analyses showed that the production of the mineral compositions was affected by the admixture mixing conditions. Therefore, the internal pore structure of the hardened matrix was investigated according to the admixture mixing conditions. The pore distribution analysis (Fig. 9) showed that the pore size was decreased with curing was increased, regardless of the admixture mixing conditions. This may be because of the production of compounds by carbonation and hydration reactions, as shown by the previous analytical results, and the crystal growth, which densifies the inside of the hardened matrix [5]. The pore size was smaller and the pore size distribution was narrower in the samples prepared by mixing only SF (Fig. 9(a)) than in the samples prepared by mixing SF and gypsum together (Fig. 9(b)), which may be related to the quantity of the hydration and carbonation products.

Fig. 10 shows the results of the compressive strength. At the curing 7 days, the strength was higher mixing only SF. However, the strength was decreased at an SF content of 20% or higher after curing 28 days, which may be due to the quantity of the hydration and

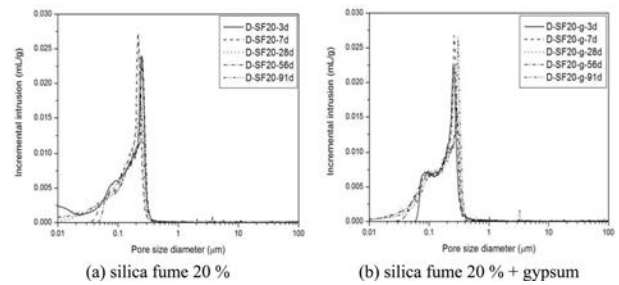


Fig. 9. Pore size distribution of Mg-based hydraulic lime containing silica fume and gypsum.

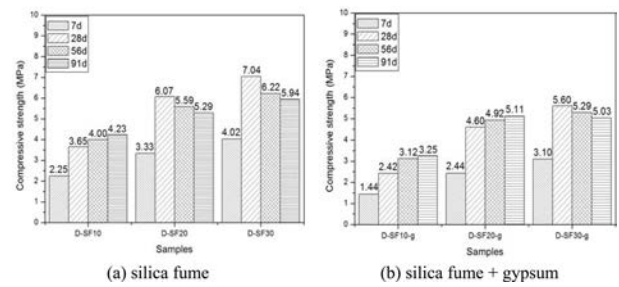


Fig. 10. Compressive strength of Mg-based hydraulic lime mortar containing silica fume and gypsum.

carbonation products as well as the interaction between the remaining SF particles.

The samples prepared by mixing only SF (Fig. 10(a)) showed higher compressive strength than the samples prepared by mixing SF and gypsum together (Fig. 10(b)), because the durability was improved more rapidly in the early curing. However, since the hydration and carbonation reactions occur for a long time and thus the properties are changed over a long term curing in the hydraulic lime, the hydraulic lime should be densified within the range where the pore structure inside the hardened matrix may not collapse despite the continuation of the hydration and carbonation and the crystal growth.

The DSC results showed that the peaks by the hydration and carbonation products were significantly increased from the curing 28 days. In addition, as the amount of the mixed SF was increased, the peaks representing the remaining SF were also increased. Therefore, as the growth of new compounds started in earnest from the material age of 28 days after the internal structure had been densified by the remaining SF particles, the internal pore structure inside the hardened body may have partially collapsed, resulting in the decrease of the strength [12-14].

Considering the expression and the long-term stability of the properties, the best mixing ratio was found to be 'SF 20% and gypsum 3%'. In contrast to the expectation that the remaining gypsum delaying the chemical reactions may have a negative effect on the expression of the properties, the results showed that the mixing of a large amount of SF may contribute to the long-term stability of the properties.

Conclusions

1. Hydration products such as C-S-H and carbonation products such as CaCO_3 were produced by mixing SF and gypsum with the D-NHL. The mixing of the inorganic admixtures improved the expression of the properties of the D-NHL itself as well as the hydration characteristics.

2. The quantity of C-S-H and CaCO_3 production was greater in the samples prepared by mixing only SF. The pore size was smaller and the pore size distribution was narrower in the samples prepared by mixing only SF.

3. The measurement of the compressive strength showed that the compressive strength was higher in the samples by mixing only SF at the curing 28 days, which may be because of the production of C-S-H and CaCO_3 . The strength was decreased at an SF mixing ratio higher than a certain level regardless of the mixing of gypsum. Therefore, an appropriate mixing ratio should be determined by investigating the correlation between the particle size of inorganic admixtures and the reactivity.

4. Considering the long-term stability of the properties, the mixing ratio enabling the continued increase of the strength until the curing 91 days was found to be 'SF 20% and gypsum 3%'. The properties of the D-NHL may be improved by controlling the types of inorganic admixtures and the mixing ratios to increase the applicability of the D-NHL.

Acknowledgments

The present study was supported by the Ministry of

Trade Industry and Energy (MOTIE) and the Korea Institute of Energy Technology Evaluation and Planning (KETEP) (Grand No. 2013T100100021).

References

1. L. Chever, S. Pavi'a and R. Howard, *Mater. Struct.* [43] (2010) 283-296.
2. BS EN 459-1:2010, Building lime, Part 1: Definitions, specifications and conformity criteria. UK: British-Adopted European Standard (2015).
3. A. El-Turki, R.J. Ball and G.C. Allen, *J. Cem. Concr. Res.* 37(2007) 1233-1240.
4. R. Chan, V. Bindiganavile, *Mater. Struct.* 10 [43] (2010) 1435-1444.
5. E. Despotou, T. Schlegel, A. Shtiza, F. Verhelst, 9th International Masonry Conference, July 2014, p.1-12.
6. J. Lanas and J.I. Alvarez, *Thermochim. Acta*, 1-2 [423] (2004) 1-12.
7. S. Pavia, B. Fitzgerald and R. Howard, *WIT Trans. Built. Env.* [83] (2005) 375-384.
8. K.Y. Moon, M.K. Choi, J.S. Cho, K.H. Cho, J.W. Ahn, *J. Korean Ceram. 2* [53] (2016) 206-214.
9. J. Y. Kim, S. K. Yum, D. W. Yoo, H. K. Choi, *J. Korean Chem. Soc.*5 [47] (2010) 357-364.
10. J. H. Ryu, G. Y. Kim, Y. K Koh, J. W. Choi, *J. Mineral Soc Korea.* 2 [23] (2010) 151-159.
11. M.W. Lee, in "An experimental study on durability analysis of mortars with anhydrite" (Konkuk University Press, 2011) p.29-30.
12. E. Adham A, *Concrete Research Letters (CRL)*, 4 [3] (2012) 528-540.
13. F. Pacheco Torgal, S. Miraldo, J.A. Labrincha, J. De Brito, *Constr. Build Mater.* [36] (2012) 141-150.
14. V.M. Sounthararajan, K. Srinivasan, A. Sivakumar, *Res. J. App. Sci. Eng. Technol.*6 [14] (2013) 2649-26.